Tailoring Magnetic Interlayer Coupling in $La_{0.7}Sr_{0.3}MnO_3/SrRuO_3$ Superlattices

M. Ziese,[1] I. Vrejoiu,[2] E. Pippel,[2] P. Esquinazi,[1] D. Hesse,[2] C. Etz,[2] J. Henk,[2] A. Ernst,[2] I. V. Maznichenko,[3] W. Hergert,[3] and I. Mertig[2,3]

[1]*Abteilung Supraleitung und Magnetismus, Universität Leipzig, D-04103 Leipzig, Germany*
[2]*Max-Planck-Institut für Mikrostrukturphysik, Weinberg 2, D-06120 Halle, Germany*
[3]*Institut für Physik, Martin-Luther-Universität Halle-Wittenberg, D-06099 Halle, Germany*

(Received 5 October 2009; published 21 April 2010)

The magnetic interlayer coupling in $La_{0.7}Sr_{0.3}MnO_3/SrRuO_3$ superlattices was investigated. High quality superlattices with ultrathin $La_{0.7}Sr_{0.3}MnO_3$ and $SrRuO_3$ layers were fabricated by pulsed laser deposition. The superlattices grew coherently with Mn/Ru intermixing restricted to about one interfacial monolayer. Strong antiferromagnetic interlayer coupling depended delicately on magnetocrystalline anisotropy and intermixing at interfaces. *Ab initio* calculations elucidated that the antiferromagnetic coupling is mediated by the Mn—O—Ru bond. The theoretical calculations allowed for a quantitative correlation between the total magnetic moment of the superlattice and the degree of Mn/Ru intermixing.

DOI: 10.1103/PhysRevLett.104.167203 PACS numbers: 75.70.Cn, 68.37.−d, 75.47.Lx, 75.60.−d

Manganites have proven to be a model system for the study of strongly correlated oxides, since their electronic and magnetic properties are very sensitive to crystal symmetry and strain. In addition, the manganite interface chemistry with its intermixing and phase separation [1,2] makes it difficult in general to realize a robust magnetic interlayer coupling between manganite layers and other oxides [3–6]. The key to a successful tailoring of the physical properties of manganite superlattices and heterostructures lies in a quantitative understanding and control of interface properties. In this work the magnetic properties of $La_{0.7}Sr_{0.3}MnO_3$ (LSMO) and $SrRuO_3$ (SRO) superlattices (SLs) were investigated. Bulk LSMO is a double exchange and SRO an itinerant ferromagnet with Curie temperatures of 370 and 150 K, respectively. The aim of this work is an understanding of the interplay between antiferromagnetic interlayer coupling, magnetocrystalline anisotropy, and interfacial quality in superlattices with ultrathin layers by combining state-of-the-art thin film fabrication and characterization techniques with *ab initio* calculations. In particular, the impact of intermixing effects at the interfaces on the magnetic properties was studied and analyzed within a realistic theoretical model.

The superlattices were fabricated by pulsed laser deposition (KrF laser) on vicinal $SrTiO_3$ (100) substrates that had atomically flat top surfaces with uniform TiO_2 termination and terrace morphology (typically 150–400 nm terrace width). All the superlattices were grown in the same conditions, at 650 °C in 0.14 mbar O_2. The microstructure of the SLs was investigated by Z contrast scanning transmission electron microscopy (Z STEM) in a TITAN 80–300 FEI microscope, and energy dispersive x-ray spectroscopy (EDX) as well as electron energy loss spectroscopy (EELS) were performed with atomic resolution, in order to probe the atomic structure of the interfaces and check for chemical interdiffusion.

Three $[LSMO/SRO]_{15}$ superlattices with fixed LSMO layer thickness of 1.6 nm (four unit cells) and various SRO layer thicknesses of 3.0, 5.0, and 8.0 nm were studied; the superlattices are denoted by SL1.6/3.0, etc. Further, a $[LSMO/STO/SRO/STO]_{10}$ superlattice with intermediate $SrTiO_3$ (STO) layers was investigated; this superlattice had layer thicknesses of 2 nm (LSMO), 7 nm (SRO), and 2 nm (STO), respectively. The magnetic properties of the superlattices were investigated by SQUID magnetometry. The magnetic moments were normalized to the LSMO volume only and were expressed in Bohr magneton per Mn ion; from this the magnetic moments per Ru in the SRO layers can be easily calculated.

Figure 1 shows a Z-STEM micrograph taken on sample SL1.6/5.0, imaging the interfaces between the LSMO layer and the two adjacent thin SRO layers. In the graph beneath the micrograph, the intensity scan along the oblique line crossing the LSMO layer and its two interfaces with the SRO layers is displayed. Based on the intensities which are monotonic functions of the atomic number Z, the atoms could be assigned and a model for the structure at the interfaces could be proposed. From that Z proportional contrast it can be deduced that an interdiffusion of Mn and Ru as well as of La and Sr proceeds gradually between at least two lattice planes, with only a slight asymmetry along the interfaces. The same behavior was also confirmed by EDX measurements. Further extensive structural characterization can be found in the supplementary online material [7].

Figure 2 shows the magnetic moment vs temperature curves of the three superlattices as measured during field cooling in a field of 0.1 T applied parallel and perpendicular to the layers, respectively. The ferro- to paramagnetic transition of the LSMO layers is clearly seen at about 300 K. Below 140 K, when SRO becomes ferromagnetic, the magnetic moment decreases sharply for all in-plane and for the perpendicular-to-plane magnetization curves of

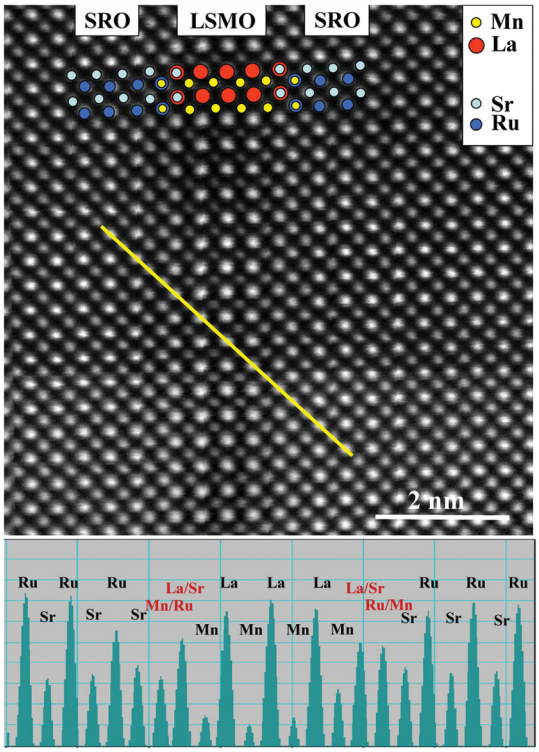

FIG. 1 (color). Upper panel: Z-STEM micrograph of sample SL1.6/5.0 showing the interfaces between a 1.6 nm LSMO layer and two adjacent 5 nm thin SRO layers. Lower panel: Intensity scan along the line indicated in the upper panel. Because of the monotonic dependence of intensity on atomic number, Mn—Ru and La—Sr interdiffusion on the scale of one to two monolayers could be deduced.

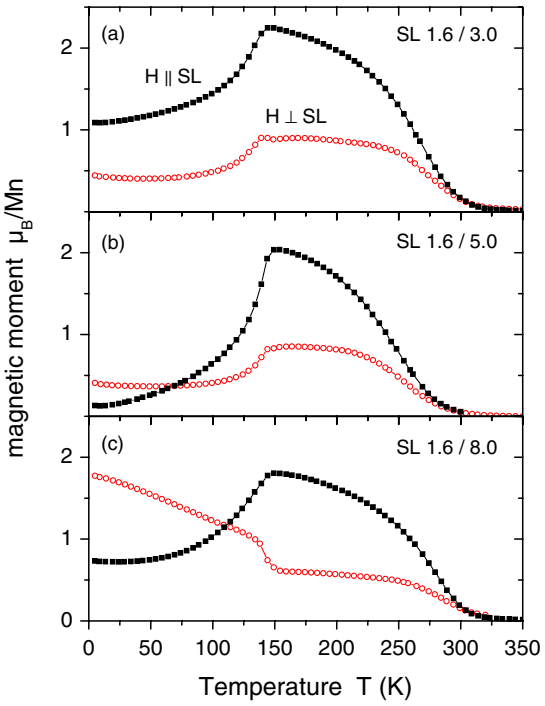

FIG. 2 (color online). Field cooled in-plane (squares) and perpendicular-to-plane (circles) magnetic moment of the three superlattices (a) SL1.6/3.0, (b) SL1.6/5.0 and (c) SL1.6/8.0 measured in a magnetic field of 0.1 T.

the two superlattices with the thinner SRO layers. These data indicate an *antiferromagnetic* coupling of the adjacent LSMO and SRO layers. Surprisingly, the perpendicular-to-plane magnetization curve of sample SL1.6/8.0 shows a *ferromagnetic* coupling of the layer magnetization. Since the magnetic moments in the perpendicular-to-plane direction above 140 K were smaller than in the in-plane direction, the magnetic hard axis of the LSMO layers is along the superlattice normal.

Figure 3 shows the corresponding magnetic moment hysteresis loops at 10 K. The curves show an astonishing evolution with the thickness of the SRO layer. Sample SL1.6/3.0 shows an in-plane magnetization curve with significant irreversibility and hysteresis loops centered at zero and high fields, whereas the perpendicular-to-plane hysteresis curve is nearly reversible and without any specific features. Since sample SL1.6/5.0 is nearly compensated at low temperatures, the central in-plane hysteresis loop is absent. In contrast superlattice SL1.6/8.0 shows more conventional hysteresis loops for both field directions.

The magnetization curves suggest the following scenario. For small SRO layer thicknesses the superlattices have an overall magnetic hard axis along the superlattice normal that enforces an in-plane orientation of the total magnetic moment. There is a strong antiferromagnetic interlayer coupling as evidenced by both temperature and field dependent magnetization data. Starting from saturation the in-plane hysteresis loop of sample SL1.6/3.0 shows a loop shift of the SRO layers of about 4 T. This is more than 2 orders of magnitude larger than the loop shifts observed in [4,5], but also corresponds to positive exchange bias. Superlattice SL1.6/5.0 shows similar behavior, but with a loop shift of about 2 T; in this case, however, the layer magnetizations from the LSMO and SRO layers nearly compensate each other such that a vortexlike hysteresis loop emerges. The perpendicular-to-plane hysteresis loops of these two samples are dominated by magnetization rotation.

Sample SL1.6/8.0 shows a different behavior. In this context one might recall that single LSMO layers on STO (001) have tetragonal symmetry with the magnetic easy axis along [110] [8]. SRO films grown on STO (001), however, have orthorhombic symmetry and a magnetic easy axis close to the surface normal [9,10]. The magnetization data indicate that sample SL1.6/8.0 is in a canted state such that the projection of the layer magnetizations on an in-plane field direction yields an apparent antiferromagnetic coupling, whereas the corresponding projection on a perpendicular-to-plane field direction yields an apparent ferromagnetic coupling. The hysteresis loops are dominated by the SRO layers. Thus, in these superlattices there is a delicate interplay between the exchange bias, the anisotropy and the applied field. A spin reorientation transition occurs at SRO layer thicknesses between 5 and 8 nm.

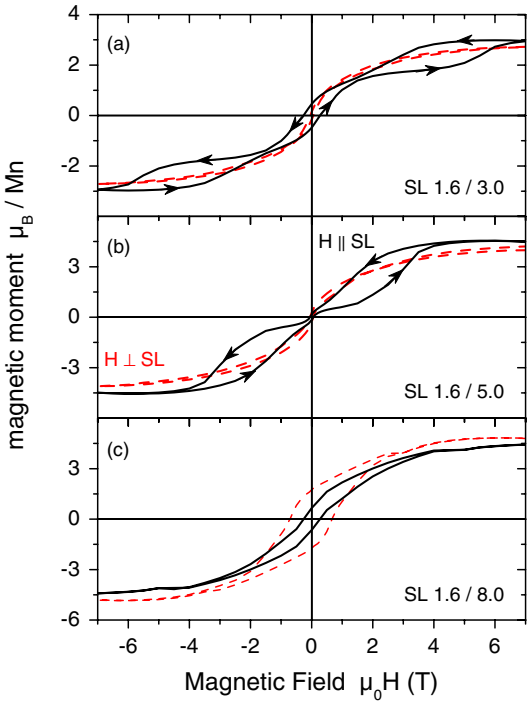

FIG. 3 (color online). In-plane (black solid lines) and perpendicular-to-plane (red dashed lines) magnetic moment hysteresis loops of the three superlattices (a) SL1.6/3.0, (b) SL1.6/5.0 and (c) SL1.6/8.0 measured at 10 K.

A 2 nm thin STO spacer in between the LSMO and SRO layers suppressed any antiferromagnetic interlayer coupling, indicating that this proceeds via direct exchange paths. Note that the LSMO layers in the superlattices still showed clear ferromagnetic order; this is in strong contrast to LSMO single layers, where orbital and antiferromagnetic order sets in already for thicknesses below 10 unit cells [11,12].

In order to elucidate the experimental results, an extensive first-principles study of the interlayer coupling in LSMO/SRO superlattices was performed. For the simulations, the Korringa-Kohn-Rostoker (KKR) Green function method within density functional theory was used. The solid solution formed between La and Sr in LSMO and the disorder effects at the LSMO/SRO interface were described by means of the coherent-potential approximation (CPA) as formulated in multiple scattering theory.

For a correct treatment of the strongly localized $3d$ electrons of Mn in LSMO the self-interaction corrected local spin density approximation (SIC-LSDA) was applied [13]. The valency of Mn was found to be Mn^{4+} in the metallic ferromagnetic phase, in agreement with [14]. This configuration was used in the present calculations. In SRO the $4d$ states are quite extended and do not need to be corrected with the SIC-LSDA. Nevertheless, electron-electron correlations can play an important role in this material [15]. By means of the generalized gradient approximation (GGA) for the exchange-correlation functional we could reproduce the experimental values for the Curie temperature in SRO. In the present work T_C was estimated by the random phase approximation.

It is known that the electronic and magnetic properties of LSMO and SRO are extremely sensitive to the crystal structure [14–16]. But an *ab initio* search of the equilibrium lattice constants is very demanding because of the large number of atoms per unit cell. The crystalline structure of the superlattice can differ significantly from the bulk one and there are no experimental data available that can unambiguously assign the correct geometry of the supercell. Hence, a reasonable approach is to deduce the layer structure indirectly via the Curie temperatures [17,18]. The first-principles determination of the Curie temperature was performed for various bulk LSMO and SRO structures adapted to the 2D lattice of the STO substrate.

The result of these calculations is listed in Table I. The best agreement between theory and experiment was achieved when LSMO and SRO were in their natural bulk structures with the 2D unit cell adapted to the STO substrate. In this case the calculated critical temperatures of 388 K for LSMO and 120 K for SRO are very close to their experimental bulk values of 370 and 150 K, respectively. Therefore, we can conclude that LSMO and SRO are grown in their bulk structure with the 2D unit cell adapted to the STO substrate.

The magnetic coupling at the LSMO/SRO interface was investigated in the SL1.6/5.0 superlattice, because of the vanishing magnetization at $T = 0$ K. This superlattice was modeled by 12 unit cells of SRO and four unit cells of LSMO. The intermixing between Mn and Ru atoms at one interface and that between La and Sr at the other, was simulated using CPA. Calculations within a relativistic KKR code showed that for the LSMO/SRO layer thickness ratio studied here the antiferromagnetic state had lowest total energy and any appreciable spin canting could be ruled out. This result is very similar to previous theoretical calculations performed for orthorhombic LSMO/SRO superlattices [19]. Besides, the total energy difference favoring antiferromagnetic coupling is robust with respect to the intermixing at the interface. Nonetheless, the Mn/Ru intermixing at the interface is crucial for the total magne-

TABLE I. Curie temperatures (T_C) of bulk LSMO and SRO (calculated using the random phase approximation) and total magnetic moment (M) per formula unit.

	Structure	T_C (K)	M (μ_B)
LSMO	cubic	610	3.53
	tetragonal	597	3.44
	rhombohedral	388	3.69
Expt.	rhombohedral	370	3.7
SRO	cubic	38	1.53
	tetragonal	66	1.65
	orthorhombic	120	1.86
Expt.	orthorhombic	150	1.6

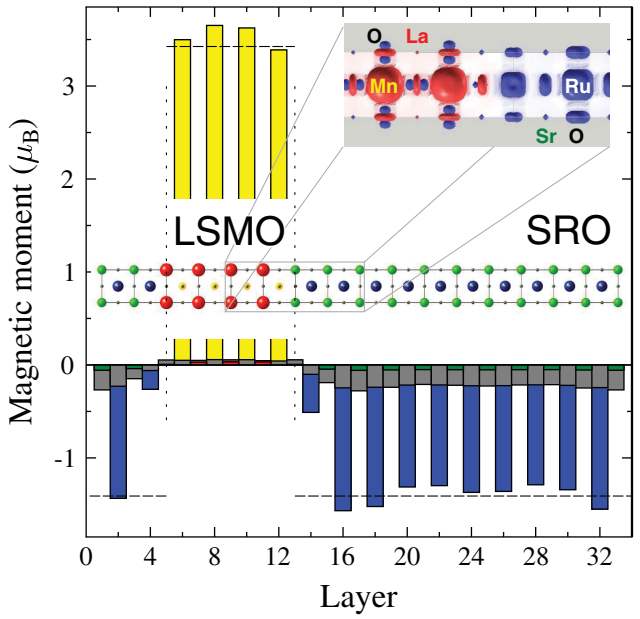

FIG. 4 (color). Calculated local magnetic moments of the LSMO/SRO SL1.6/5.0. Mn is shown in yellow, La/Sr in red, Sr in green, Ru in blue, and O in grey color. Dashed lines show bulk values of local magnetic moments on Mn and Ru in bulk LSMO and SRO, respectively. The supercell is represented in the center of the figure. Inset: spin density at the interface. Positive and negative spin densities are represented in red and blue, respectively.

tization of the superlattice. Figure 4 shows layer and atomically resolved magnetic moments in the SL1.6/5.0 superlattice with ideal interfaces in the case of antiferromagnetic coupling. Although the magnetic moments of the SRO layers are substantially reduced at the interface, there is no compensation of the magnetization between the SRO and the LSMO multilayers. Still the net magnetization of 12 SRO layers is larger than the magnetization of four LSMO layers. The total magnetic moment of about $1\mu_B$/Mn is not small enough to reproduce the experimental results. This discrepancy can be reduced by intermixing of Mn and Ru atoms at one of the interfaces. As a consequence, the magnetic moments of the interfacial Ru atoms decrease drastically, leading to an almost nonmagnetic component, whereas the Mn moments are only slightly affected. The total moment can be reduced to less than $0.2\mu_B$/Mn for a Mn concentration of 70% at the interface.

Thus, the experimental finding of Mn/Ru intermixing in the first atomic layer at the LSMO/SRO interface was confirmed and, moreover, an estimation of its concentration was possible. It was further found that oxygen vacancy concentrations up to 10% hardly affected the magnetic moments; the influence of 10% expansion (compression) of the lattice spacing marginally affected the magnetic moment of the RuO_2-terminated interface whereas it increases (decreases) by $0.25\mu_B$/Mn at the SrO-terminated interface.

As mentioned above, the total energy calculations indicated a lower energy for the antiferromagnetic coupling between LSMO and SRO. In this energy gain, interfacial oxygen atoms play a very important role [19]. In SRO the spin density is prevalently of the same sign, while in LSMO it alternates in sign along Mn—O bonds (see inset to Fig. 4). At the interface, the oxygen ions are strongly polarized by the Mn atoms, leading to an asymmetry in the spin density. Induced by the negative spin density of the σ bond at the interface, the Ru atoms adjust their moments in parallel direction and, therefore, the SRO magnetization is oppositely aligned with respect to the LSMO magnetization.

In summary, it was shown that strong antiferromagnetic interlayer coupling can be created in LSMO/SRO superlattices with ultrathin individual layers. *Ab initio* calculations showed that the antiferromagnetic interlayer coupling is mediated by the Mn—O—Ru bond. The total magnetic moment of the superlattices depends on the thickness ratio of the individual layers as well as on the Mn/Ru intermixing at the interface. By a combination of structural techniques and magnetometry as well as theoretical calculations, the degree of Mn/Ru interdiffusion could be quantitatively determined and its impact on the magnetic properties could be evaluated.

This work was supported by the DFG within the Collaborative Research Center SFB 762 "Functionality of Oxide Interfaces." The calculations were performed at the John von Neumann Institute in Jülich and Rechenzentrum Garching of the Max Planck Society (Germany).

[1] M.-H. Jo *et al.*, Phys. Rev. B **61**, R14 905 (2000).
[2] M. Bibes *et al.*, Phys. Rev. Lett. **87**, 067210 (2001).
[3] I. N. Krivorotov *et al.*, Phys. Rev. Lett. **86**, 5779 (2001).
[4] X. Ke *et al.*, Appl. Phys. Lett. **84**, 5458 (2004).
[5] X. Ke *et al.*, J. Appl. Phys. **97**, 10K115 (2005).
[6] P. Padhan, W. Prellier, and R. C. Budhani, Appl. Phys. Lett. **88**, 192509 (2006).
[7] See supplementary material at http://link.aps.org/supplemental/10.1103/PhysRevLett.104.167203.
[8] M. Ziese, Phys. Status Solidi B **242**, R116 (2005).
[9] Q. Gan *et al.*, J. Appl. Phys. **85**, 5297 (1999).
[10] S. Kolesnik *et al.*, J. Appl. Phys. **99**, 08F501 (2006).
[11] Z. Fang, I. V. Solovyev, and K. Terakura, Phys. Rev. Lett. **84**, 3169 (2000).
[12] M. Huijben *et al.*, Phys. Rev. B **78**, 094413 (2008).
[13] M. Lüders *et al.*, Phys. Rev. B **71**, 205109 (2005).
[14] G. Banach and W. M. Temmerman, Phys. Rev. B **69**, 054427 (2004).
[15] J. M. Rondinelli *et al.*, Phys. Rev. B **78**, 155107 (2008).
[16] V. Krayzman *et al.*, AIP Conf. Proc. **882**, 431 (2007).
[17] I. D. Hughes *et al.*, Nature (London) **446**, 650 (2007).
[18] G. Fischer *et al.*, Phys. Rev. B **80**, 014408 (2009).
[19] Y. Lee, B. Caes, and B. Harmon, J. Alloys Compd. **450**, 1 (2008).